Progress in Fractional Differentiation and Applications
An International Journal

http://dx.doi.org/10.18576/pfda/110407

Numerical and Dynamical Analysis of an Infectious Disease Epidemic Model Through Fractional Derivative

Mohamed A. Hafez [1,2], *Montasir Qasymeh* [3], *Zafar Iqbal* [4], *Nauman Ahmed* [4], *Ali Akgül* [5,6,*], *and Betty Wan Voon* [7]

[1] Faculty of Engineering and Quantity Surviving, INTI International University Colleges, Nilai, Malaysia
[2] Faculty of Management, Shinawatra University, Pathum Thani, Thailand
[3] Electrical and Computer Engineering Department, Abu Dhabi University, Abu Dhabi, United Arab Emirates
[4] Department of Mathematics and Statistics, The University of Lahore, Lahore, Pakistan
[5] Department of Electronics and Communication Engineering, Saveetha School of Engineering, SIMATS, Chennai, Tamilnadu, India
[6] Department of Mathematics, Art and Science Faculty, Siirt University, 56100 Siirt, Turkey
[7] Department of Civil Engineering, (COE), Universiti Tenaga Nasional, Kajang, Malaysia

Received: 30 Oct. 2024, Revised: 24 Apr. 2024, Accepted: 3 Jun. 2025
Published online: 1 Oct. 2025

Abstract: Nipah virus infection is a dreadful disease for human lives. In this work, an integer order model of Nipah virus transmission is converted into a fractional order model by using Caputo fractional differential operator for a more realistic approach to the disease transmission phenomena. On that account, the projected fractional model is dealt with analytically and numerically. The continuous system has two states of dynamic disease equilibrium i.e. disease-free state and endemic state. Moreover, the underlying system has a unique solution. The positivity and the boundedness of the fractional system are thoroughly investigated. The basic reproduction number R0 is worked out mathematically. The contribution of basic reproductive number R0 in stability analysis and disease dynamics is explored. The nonstandard numerical scheme is developed for finding the approximate solutions of the fractional system. The salient features of the state variables are examined to measure the efficacy of the numerical method. The article is closed by enlisting some productive and novel outcomes of the study.

Keywords: Fractional epidemic model; Nipah virus (NVD); LaSalle Principal; GL non-standard finite difference schemes.

1 Introduction

The Nipah virus disease (NVD) is an infectious viral infection caused by the Nipah virus. This virus is a member of the Paramyxoviridae family and Hanipavirus genus. This virus was originated in the Sungai Nipah, a Malaysian village during the sudden appearance of encephalitis and respiratory disease, in 1998. The transmission of the Nipah virus (NV) involves animals and humans i.e., it is a zoonotic infection. The people with respiratory and neurological issues are the easy target for NVD. It can be characterized as an acute and systematic animal disease that is ultimately transmitted to humans. Approximately two-third of noxious.. microorganism that has been recently discovered, arise from wildlife and in round numbers 75% of these pathogens are transmitted through animals [1]. The NVD may create the fatal and severe health issues. The laboratory test and techniques reflected that the NVD infected the neurological and respiratory system in pig [3]. The frugivorous bats that are also known as flying foxes or fruit bats are the main source of NVD transmission. This infection is highly infectious and can be spread through the infected animals in the vicinity. Generally, the outbreaks of NVD have been observed in the area where the infection carrier bats existed. For instance, Bangladesh, Malaysia, Singapore and India as well as many cases have been reported in Philippines. The outbreaks of the NVD and spread of NV from animal to human is connected to the reduction in bats' environment [4].

There are many modes of transmission including Pteropas-swine-man virus dynamics, spread of infection through the consumption of infected food by humans, human to human direct transmission and transfer of NV from bats to human are considered. The effective measure for epidemic in pig are isolation, travel restrictions and massacre of infected pigs [5,6]. A reliable diagnostic test may be adopted by applying molecular techniques, but serological tests are also effective.

* Corresponding author e-mail: aliakgul00727@mail.com

Since bats are the main source of the NV spread, so reducing exposure to either NV or bats is the best strategy to stop the new occurrence of the NVD, even if the treatment options are being explored [5]. Currently, there is no effective treatment or vaccine for the NVD, more studies are needed for fully understanding the relationship between NV and therapeutic reactions. The adequate preventive measures, vicinity and curative treatment are required to control the infection. The main objective for developing a range of vaccines by using Nipah virus immunogenic proteins or peptides is their purported immunogenicity or their capability to elicit a neutralizing antibody response. These vaccines should have the potential to quickly neutralize the infection and establish a cell mediated response to clear the virus. To measure the efficacy of the NV is a challenging task due to its high pathogenicity and issues associated with its usage [7,9]. Despite everything, some laboratory vaccines triggered a reaction various level of clinical protection [3,10,13]. Furthermore, a deep understanding of the ecological distribution of source bats in environment would play a vital role in preventing and controlling the disease dynamics [4]. For Hi-techs like remote sensing and geography information systems are the significant devices for detecting the animal proportions to the habitat and NV in wildlife [14,15], by taking into account the key features of the fruit bats areas which are responsible for the NV spread in the region [4,16].

However, that climate change which rise the temperature extremely in tropical areas has a terrible impact on the flexibility of flying horses to the hot weather conditions. This fact is true for survival of the species and demography. It is also in line with the spread of NV [17,19]. The pertinent law in Europe is force in the general framework of zoonotic disease and disease control. Following NV outbreaks in pig, Malaysia implemented strict biosecurity measures to stop the infection from spreading. This security infected if yes sections on the pig and meet trade construction of an infected and safety areas near the outbreak Myers of infected pigs and emphasizes its transmission dynamics, diagnostic techniques, and preventive strategies aiming to raise awareness and enhance efforts to combat this neglected zoonotic disease [2,21, 27]. The Indian National Centre for disease control (NCDC) established the criteria for classifying the different stages of the infection in the population. The basic aim of these efforts is to control and slow down the virus propagation [3,22]. The appropriate printine measure for the NVD, are based on the limiting interactions with reservoir species, adoption of proper pig farming practices and focusing on the hygienic and nutritional needs of the population in the neighborhood of outbreak areas. WHO has ratified that Bangladesh faced many NVD outbreaks in various districts from 2001 to 2021. But, the clinical symptoms of the NVD in humans are very dangerous. The repetition of Nipah encephalitis gave rise to many deaths in Bangladesh [4].

A mathematical model is an appropriate tool for forecasting and understanding the propagation of the disease dynamics and it is fascinating the researcher's community gradually. In the recent past, fractional order epidemic models have got the attraction of the researchers. These models have reflected the preferences over the integer order epidemic models. As the fractional order derivatives have non-local by nature, they can measure the change-over on interval. Contrary to the integer order derivative, which are local operator and can measure the change in the neighborhood of a point. In addition, the fractional order epidemic model captures the memory effect which is in line with many biological phenomena such as disease dynamics. Moreover, these models best fit with the real data of the epidemics. Ahmed, N et.al analyzed many infectious based on fractional order epidemic model such as Covid-19 [23] etc. In this work we have extended the integer order model to the fractional order Nipah virus model. This model will help in deeply perceiving the NVD dynamics in the community. On the basis of this study, health department can predict the disease dynamics and design the strategies to control slow down and even eradicate the disease from the human population and environment.

1.1 Basic Definitions

In this preliminary section, we have basic definitions regarding fractional calculus.

1.2 Caputo Fractional Derivative

Let $Z(\tau)$ satisfy some smoothness condition in every finite interval $(0,t)$ with $t \leq \tau$. Then

$$({}_0^C)D_t^u Z(t) = \frac{1}{\Gamma(m-u)} \int_0^t (t-\tau)^{-u-1+m} \frac{d^m}{d\tau^m} Z(\tau) d\tau, \quad m-1 < u < m. \tag{1}$$

1.3 Mittag-Leffler Function

The Mittag-Leffler function is represented by $E_{\alpha,\beta}$ described below:

$$E_{\alpha,\beta}(s) = \sum_{k=0}^{\infty} \frac{s^k}{\Gamma(\alpha k+\beta)}, \quad \alpha \in \mathbb{R}^+, s \in \mathbb{C}. \tag{2}$$

2 Fractional Model

The parameters and variables of Nipah disease are defined as follows, for any random time t, $S(t)$ stands for the population at risk for catching the Nipah virus, people who were exposed to the Nipah virus but were not infected are defined by $E(t)$. $R(t)$ stands for those individuals who are Nipah virus-free. Λ is the number of susceptible individuals starting with the birth rate, β describes the rate of contact, α denotes the infection's rate of progression, δ denotes the prevalence of disease-related deaths, μ represents rate of death naturally, ε_1 represents the percentage of exposed people who recover after becoming aware, ε_2 represents the percentage of infected people who have recovered after treatment, η stands for the individuals under quarantine, τ stands for the available centers of isolation. γ stands for improved personal hygiene brought on by increased public awareness, σ for the rate of public awareness, and λ for surveillance coverage. The fractional order model's governing equations are as follows [24]:

$$({}_0^C)D_t^{\xi} S(t) = \Lambda - \beta(1-\eta\lambda\gamma)(1-\gamma\lambda\alpha)\frac{IS}{N} - \mu S, \tag{3}$$

$$({}_0^C)D_t^{\xi} E(t) = \beta(1-\eta\lambda\gamma)(1-\gamma\lambda\alpha)\frac{IS}{N} - \alpha E - \varepsilon_1 E - \mu E, \tag{4}$$

$$({}_0^C)D_t^{\xi} I(t) = \alpha E - \varepsilon_2 I - \delta I - \mu I, \tag{5}$$

$$({}_0^C)D_t^{\xi} R(t) = \varepsilon_1 E + \varepsilon_2 I - \mu R. \tag{6}$$

With initial conditions

$$S(0) = S_0 \geq 0, \quad E(0) = E_0 \geq 0, \quad I(0) = I_0 \geq 0, \quad R(0) = R_0 \geq 0.$$

2.1 Steady States of NV Model

The Nipah virus infection model (3)-(6) exhibits steady states as follows: infection-free steady state (IFSS) $= \left(\frac{\Lambda}{\mu}, 0, 0, 0\right)$, and infection existence steady state (IESS) $= (S^1, E^1, I^1, R^1)$, where:

$$S^1 = \frac{N(\varepsilon_2+\delta+\mu)(\alpha+\varepsilon_1+\mu)}{\alpha\beta(1-\eta\lambda\tau)(1-\gamma\lambda\sigma)},$$

$$E^1 = \frac{\Lambda\alpha\beta(1-\eta\lambda\tau)(1-\gamma\lambda\sigma)(\varepsilon_2+\delta+\mu) - \mu N(\alpha+\varepsilon_1+\mu)(\varepsilon_2+\delta+\mu)^2}{\alpha\beta(1-\eta\lambda\tau)(1-\gamma\lambda\sigma)(\varepsilon_2+\delta+\mu)(\alpha+\varepsilon_1+\mu)},$$

$$I^1 = \frac{\Lambda\alpha\beta(1-\eta\lambda\tau)(1-\gamma\lambda\sigma) - \mu N(\varepsilon_2+\delta+\mu)(\alpha+\varepsilon_1+\mu)}{\beta(1-\eta\lambda\tau)(1-\gamma\lambda\sigma)(\varepsilon_2+\delta+\mu)(\alpha+\varepsilon_1+\mu)},$$

$$R^1 = \frac{\Lambda\alpha\beta\varepsilon_1(1-\eta\lambda\tau)(1-\gamma\lambda\sigma)(\varepsilon_2+\delta+\mu) - \mu N\varepsilon_1(\alpha+\varepsilon_1+\mu)(\varepsilon_2+\delta+\mu)^2}{\alpha\beta\mu(1-\eta\lambda\tau)(1-\gamma\lambda\sigma)(\varepsilon_2+\delta+\mu)(\alpha+\varepsilon_1+\mu)}$$
$$+ \frac{\Lambda\alpha\beta\varepsilon_2(1-\eta\lambda\tau)(1-\gamma\lambda\sigma) - \varepsilon_2\mu N\alpha(\varepsilon_2+\delta+\mu)(\alpha+\varepsilon_1+\mu)}{\alpha\beta\mu(1-\eta\lambda\tau)(1-\gamma\lambda\sigma)(\varepsilon_2+\delta+\mu)(\alpha+\varepsilon_1+\mu)}.$$

2.2 Positivity and Boundedness

In this section we have shown that the solutions of the system (3)-(6) are bounded and positive.

Theorem 1. *For the initial condition, $S(0) = S_0 > 0$, $E(0) = E_0 > 0$, $I(0) = I_0 > 0$, $R(0) = R_0 > 0$, the solution of system is bounded.*

Proof. Let us consider the expression below:

$$({}_0^C)D_t^{\xi} N(t) = ({}_0^C)D_t^{\xi} S(t) + ({}_0^C)D_t^{\xi} E(t) + ({}_0^C)D_t^{\xi} I(t) + ({}_0^C)D_t^{\xi} R(t),$$

$$({}_0^C)D_t^{\xi} N(t) = \Lambda - \mu(S+E+I+R) - \delta I,$$

$$({}_0^C)D_t^{\xi} N(t) + \mu N(t) = \Lambda - \delta I,$$

$$({}_0^C)D_t^{\xi} N(t) + \mu N(t) \leq \Lambda.$$

By Laplace transformation:

$$\begin{aligned}\mathscr{L}\{({}_0^C)D_t^{\xi}N(t)\}+\mu\mathscr{L}\{N(t)\}&\leq\Lambda\mathscr{L}\{1\},\\(s^{\xi}+\mu)\mathscr{L}\{N(t)\}&\leq\Lambda\cdot\frac{1}{s}+s^{\xi-1}N(0),\\\mathscr{L}\{N(t)\}&\leq\frac{s^{\xi-1}N(0)}{s^{\xi}+\mu}+\frac{\Lambda}{s(s^{\xi}+\mu)}.\end{aligned}$$

Let $M_1=\mu$:

$$\begin{aligned}\mathscr{L}\{N(t)\}&\leq\frac{s^{\xi-1}N(0)}{s^{\xi}+M_1}+\frac{\Lambda s^{-1}}{s^{\xi}+M_1},\\&\leq\frac{\Lambda s^{\xi-(1+\xi)}}{s^{\xi}+M_1}+\frac{s^{\xi-1}N(0)}{s^{\xi}+M_1}.\end{aligned}$$

By Laplace inverse:

$$\begin{aligned}N(t)&\leq\mathscr{L}^{-1}\left\{\frac{\Lambda s^{\xi-(1+\xi)}}{s^{\xi}+M_1}\right\}+\mathscr{L}^{-1}\left\{\frac{s^{\xi-1}N(0)}{s^{\xi}+M_1}\right\},\\&\leq\Lambda t^{\xi}E_{\xi,1+\xi}(-M_1t^{\xi})+N(0)E_{\xi,1}(-M_1t^{\xi}),\\&\leq\mu\cdot\frac{\Lambda}{\mu}t^{\xi}E_{\xi,1+\xi}(-M_1t^{\xi})+N(0)E_{\xi,1}(-M_1t^{\xi}).\end{aligned}$$

Let $M=\max\{N(0),\frac{\Lambda}{\mu}\}$:

$$\begin{aligned}N(t)&\leq M\left\{\mu t^{\xi}E_{\xi,1+\xi}(-M_1t^{\xi})+E_{\xi,1}(-M_1t^{\xi})\right\},\\&\leq M\left\{\mu t^{\xi}E_{\xi,1+\xi}(-M_1t^{\xi})-\mu t^{\xi}E_{\xi,1+\xi}(-M_1t^{\xi})+\frac{1}{\Gamma(1)}\right\},\\&\leq M.\quad\because\Gamma(1)=1\end{aligned}$$

Lemma 1.*For any initial positive values, then equation (3)-(6) is positive invariant in* $\mathbb{R}^4_+$.

*Proof.*Consider the equation (3):

$$({}_0^C)D_t^{\xi}S\big|_{S=0}=\Lambda\geq 0.$$

From equation (4):

$$({}_0^C)D_t^{\xi}E\big|_{E=0}=\beta(1-\eta\lambda\gamma)(1-\gamma\lambda\alpha)\frac{IS}{N}\geq 0.$$

From equation (5) we reach at:

$$({}_0^C)D_t^{\xi}I\big|_{I=0}=\alpha E\geq 0.$$

From equation (6) we get:

$$({}_0^C)D_t^{\xi}R\big|_{R=0}=\varepsilon_1E+\varepsilon_2I\geq 0.$$

As desired.

2.3 Uniqueness and Existence

Here we will present the existence and uniqueness of the system (3)-(6).

Theorem 2.*For every time t, the solution of the fractional model will exist and the solution will also be unique.*

*Proof.*Let $K(S) = \Lambda - \beta(1-\eta\lambda\gamma)(1-\gamma\lambda\alpha)\frac{IS}{N} - \mu S$,

$$\begin{aligned}
\|K(S_1) - K(S_2)\| &= \left\| \Lambda - \beta(1-\eta\lambda\gamma)(1-\gamma\lambda\alpha)\frac{I}{N}S_1 - \mu S_1 - \Lambda + \beta(1-\eta\lambda\gamma)(1-\gamma\lambda\alpha)\frac{I}{N}S_2 + \mu S_2 \right\|, \\
&\leq \left\| \beta(1-\eta\lambda\gamma)(1-\gamma\lambda\alpha)\frac{I}{N}(S_2 - S_1) \right\| + \|\mu(S_2 - S_1)\|, \\
&\leq \frac{\beta(1-\eta\lambda\gamma)(1-\gamma\lambda\alpha)}{N}\|I\|\|S_2 - S_1\| + \mu\|S_2 - S_1\|, \\
&\leq \left(\frac{\beta(1-\eta\lambda\gamma)(1-\gamma\lambda\alpha)}{N}\|I\| + \mu \right) \|S_2 - S_1\|, \\
&\leq \left(\frac{\beta(1-\eta\lambda\gamma)(1-\gamma\lambda\alpha)}{N}N_1 + \mu \right) \|S_2 - S_1\|, \quad (\because \|I\| = N_1 \text{ (say)})
\end{aligned}$$

Therefore, $K(S)$ satisfies the Lipschitz condition. For contraction mapping:

$$\frac{\beta(1-\eta\lambda\gamma)(1-\gamma\lambda\alpha)}{N}N_1 + \mu < 1.$$

Similarly, for the rest of the equations we have:

$$\begin{aligned}
F_1 &= \frac{\beta(1-\eta\lambda\gamma)(1-\gamma\lambda\alpha)}{N}N_1 + \mu, \\
F_2 &= \alpha + \varepsilon_1 + \mu, \\
F_3 &= \varepsilon_2 + \delta^{\xi} + \mu, \\
F_4 &= \mu.
\end{aligned}$$

Let $F = \max\{F_1, F_2, F_3, F_4\}$, therefore:

$$\begin{aligned}
\|K(S_1) - K(S_2)\| &\leq F\|S_1 - S_2\|, \\
\|M(E_1) - M(E_2)\| &\leq F\|E_1 - E_2\|, \\
\|N(I_1) - N(I_2)\| &\leq F\|I_1 - I_2\|, \\
\|L(R_1) - L(R_2)\| &\leq F\|R_1 - R_2\|.
\end{aligned}$$

For $F < 1$, $K(S), M(E), N(I)$ and $L(R)$ are contraction mappings.

2.4 Local Stability

Local stability of the system (3)-(6) is presented here with the help of the Jacobian matrix theory.

Theorem 3.*The steady-state solution IFSS of the fractional Nipah virus model is locally asymptotically stable (LAS) if* $R_0 < 1$.

*Proof.*Considering the Jacobian at IFSS:

$$\left| J\left(\frac{\Lambda}{\mu}, 0, 0, 0\right) - \lambda I \right| = \begin{vmatrix} -\mu - \lambda & 0 & -\frac{\beta(1-\eta\lambda\tau)(1-\gamma\lambda\sigma)\Lambda}{\mu N} & 0 \\ 0 & -(\alpha + \varepsilon_1 + \mu) - \lambda & \frac{\beta(1-\eta\lambda\tau)(1-\gamma\lambda\sigma)\Lambda}{\mu N} & 0 \\ 0 & \alpha & -(\varepsilon_2 + \delta + \mu) - \lambda & 0 \\ 0 & \varepsilon_1 & \varepsilon_2 & -\mu - \lambda \end{vmatrix} = 0$$

Eigenvalues:

$$\begin{aligned}
\lambda_1 &= -\mu < 0, \\
\lambda_2 &= -\mu < 0,
\end{aligned}$$

The remaining eigenvalues satisfy:

$$[-(\alpha+\varepsilon_1+\mu)-\lambda][-(\varepsilon_2+\delta+\mu)-\lambda]-\alpha\left(\frac{\beta(1-\eta\lambda\tau)(1-\gamma\lambda\sigma)\Lambda}{\mu N}\right)=0$$

Let $A=(\alpha+\varepsilon_1+\mu)$, $B=(\varepsilon_2+\delta+\mu)$, $C=\alpha\left(\frac{\beta(1-\eta\lambda\tau)(1-\gamma\lambda\sigma)\Lambda}{\mu N}\right)$:

$$\lambda^2+(A+B)\lambda+AB-C=0$$

By Routh-Hurwitz criteria for 2nd order:

$$A+B>0,$$
$$AB-C>0 \quad \text{if} \quad R_0=\frac{\alpha\beta(1-\eta\lambda\tau)(1-\gamma\lambda\sigma)\Lambda}{N(\alpha+\varepsilon_1+\mu)(\varepsilon_2+\delta+\mu)\mu}<1.$$

Hence, IFSS is locally asymptotically stable (LAS).

Theorem 4.*The steady-state solution IESS of the fractional Nipah virus model is LAS if* $R_0>1$.

*Proof.*The Jacobian at IESS:

$$J=\begin{bmatrix} -\frac{\beta(1-\eta\lambda\tau)(1-\gamma\lambda\sigma)I^1}{N}-\mu & 0 & -\frac{\beta(1-\eta\lambda\tau)(1-\gamma\lambda\sigma)S^1}{N} & 0 \\ \frac{\beta(1-\eta\lambda\tau)(1-\gamma\lambda\sigma)I^1}{N} & -(\alpha+\varepsilon_1+\mu) & \frac{\beta(1-\eta\lambda\tau)(1-\gamma\lambda\sigma)S^1}{N} & 0 \\ 0 & \alpha & -(\varepsilon_2+\delta+\mu) & 0 \\ 0 & \varepsilon_1 & \varepsilon_2 & -\mu \end{bmatrix}$$

Characteristic equation:

$$\lambda^{*3}+(a_4+a_6-a_1)\lambda^{*2}-(a_1a_4-a_1a_6-a_4a_6-a_5\alpha)\lambda^*+a_1a_4a_6-a_1a_5\alpha+a_2a_3\alpha=0$$

By Routh-Hurwitz criterion for 3rd order, the system is locally asymptotically stable when $R_0>1$.

2.5 Global Stability

Here the Volterra-type Lyapunov function is used to show the global asymptotic stability.

Theorem 5.*The system is globally asymptotically stable at disease-free equilibrium point* E^0 *if* $R_0<1$.

*Proof.*Consider a Volterra-type candidate Lyapunov function:

$$G=S-S_0-S_0\ln\left(\frac{S}{S_0}\right)+E+I+R$$

Fractional derivative:

$$({}_0^C)D_t^{\xi}G(t)\le-\frac{\Lambda(S-S_0)^2}{SS_0} \quad \text{at IFSS}\left(\frac{\Lambda}{\mu},0,0,0\right)$$

By LaSalle's invariance theorem, the system is globally asymptotically stable.

Theorem 6.*The system is globally asymptotically stable at the endemic equilibrium point* E^* *if* $R_0>1$.

*Proof.*Consider a Volterra-type candidate Lyapunov function:

$$G=S-S^*-S^*\ln\left(\frac{S}{S^*}\right)+E-E^*-E^*\ln\left(\frac{E}{E^*}\right)+I-I^*-I^*\ln\left(\frac{I}{I^*}\right)+R-R^*-R^*\ln\left(\frac{R}{R^*}\right)$$

Fractional derivative:

$$({}_0^C)D_t^{\xi}G(t)\le-\frac{\Lambda(S-S^*)^2}{SS^*}-\frac{\beta(1-\eta\lambda\gamma)(1-\gamma\lambda\alpha)}{N}\frac{(E-E^*)^2}{EE^*}-\alpha E\frac{(I-I^*)^2}{II^*}-(\varepsilon_1E+\varepsilon_2I)\frac{(R-R^*)^2}{RR^*}$$

By LaSalle's invariance theorem, the system is globally asymptotically stable.

3 Numerical Modeling

In this section, we will design a numerical approach for the approximation of model (3)-(6), using GL-NSFD algorithm [25]. We have:

$$({}_0^C)D_t^{\xi} S(t) = \Lambda - \frac{\beta(1-\eta\lambda\gamma)(1-\gamma\lambda\alpha)}{N} IS - \mu S, \tag{7}$$

$$({}_0^C)D_t^{\xi} E(t) = \frac{\beta(1-\eta\lambda\gamma)(1-\gamma\lambda\alpha)}{N} IS - \alpha E - \varepsilon_1 E - \mu E, \tag{8}$$

$$({}_0^C)D_t^{\xi} I(t) = \alpha E - \varepsilon_2 I - \delta I - \mu I, \tag{9}$$

$$({}_0^C)D_t^{\xi} R(t) = \varepsilon_1 E + \varepsilon_2 I - \mu R. \tag{10}$$

From (7) we derive:

$$S_{n+1} = \frac{\phi(h)^{\xi}\Lambda + \sum_{i=1}^{n+1} p_i^{\xi} S_{n+1-i} + q_{n+1}^{\xi} S_0}{\phi(h)^{\xi}\left(\frac{\beta(1-\eta\lambda\gamma)(1-\gamma\lambda\alpha)}{N} I_n + \mu\phi(h)^{\xi}\right)}. \tag{11}$$

Similarly, we have the following results:

$$E_{n+1} = \frac{\phi(h)^{\xi}\frac{\beta(1-\eta\lambda\gamma)(1-\gamma\lambda\alpha)}{N} S_{n+1} I_n + \sum_{i=1}^{n+1} p_i^{\xi} E_{n+1-i} + q_{n+1}^{\xi} E_0}{1 + \alpha\phi(h)^{\xi} + \varepsilon_1\phi(h)^{\xi} + \mu\phi(h)^{\xi}}, \tag{12}$$

$$I_{n+1} = \frac{\alpha E_{n+1} + \sum_{i=1}^{n+1} p_i^{\xi} I_{n+1-i} + q_{n+1}^{\xi} I_0}{1 + \varepsilon_2\phi(h)^{\xi} + \delta\phi(h)^{\xi} + \mu\phi(h)^{\xi}}, \tag{13}$$

$$R_{n+1} = \frac{\varepsilon_1 E_{n+1} + \varepsilon_2 I_{n+1} + \sum_{i=1}^{n+1} p_i^{\xi} R_{n+1-i} + q_{n+1}^{\xi} R_0}{1 + \mu\phi(h)^{\xi}}. \tag{14}$$

3.1 Positivity and Boundedness of Scheme

The positivity and boundedness of the scheme is proved in this section, with the help of mathematical induction.

Theorem 7. *Suppose that S_0, E_0, I_0, R_0 are finite and positive also $S_0 + E_0 + I_0 + R_0 \leq N_0$. Also $\alpha, \beta, \mu, \lambda, \eta, \gamma, \varepsilon_1, \delta, \varepsilon_2$ are all positive then there is a constant N_n such that $S_{n+1}, E_{n+1}, I_{n+1}, R_{n+1} \leq N_n \ \forall n \in \mathbb{Z}^+$.*

Proof. Suppose that all the state variables and controlled parameters are non-negative with $S^0, E^0, I^0, R^0 \geq 0$ then $S_{n+1}, E_{n+1}, I_{n+1}, R_{n+1} \geq 0$, $\forall n \in \mathbb{Z}^+$. Consider the expression:

For $n = 0$:

$$S_1 = \frac{\phi(h)^{\xi}\Lambda + p_1 S_0 + q_1^{\xi} S_0}{\phi(h)^{\xi}\left(\frac{\beta(1-\eta\lambda\gamma)(1-\gamma\lambda\alpha)}{N} I_0 + \mu\phi(h)^{\xi}\right)}$$

Since $I_0 > 0$ with all the controlled positive parameters and $1 - \eta\lambda\gamma > 0$, $1 - \gamma\lambda\alpha > 0$, we have $S_1 > 0$.

Next we suppose that the result holds for $n = \{1, 2, 3, \ldots, n-1\}$, $S_n, E_n, I_n, R_n > 0$, $\forall n = \{1, 2, 3, \ldots, n-1\}$. Moreover, for $n \in \mathbb{Z}^+$ we have:

$$S_{n+1} = \frac{\phi(h)^{\xi}\Lambda + \sum_{i=1}^{n+1} p_i S_{n+1-i} + q_{n+1}^{\xi} S_0}{\phi(h)^{\xi}\left(\frac{\beta(1-\eta\lambda\gamma)(1-\gamma\lambda\alpha)}{N} I_n + \mu\phi(h)^{\xi}\right)}$$

Since all the discretized state variables and parameters are positive, therefore $S_{n+1} > 0$, similarly $E_{n+1} > 0$, $I_{n+1} > 0$, and $R_{n+1} > 0$.

Hence the proposed numerical scheme preserves the positivity, $\forall n \in \mathbb{Z}^+$.

Theorem 8. *Suppose that $S_0 + E_0 + I_0 + R_0 = N(N_0, \xi)$, and all the parameters are positive for $\xi \in (0, 1)$. Then there is a constant $N(N_{n+1}, \xi) = \frac{\xi + \frac{1}{\Gamma(1-\xi)} + N(N_{n+1}, \xi)}{1 + \mu^{\xi}\phi(h^{\xi})}$, such that $S_{n+1} + E_{n+1} + I_{n+1} + R_{n+1} = N(N_{n+1}, \xi)$ for $n = 0, 1, 2, 3, \ldots, N_{n+1}$.*

Proof. Adding the equations (11)-(14):

For $n=0$:

$$(S_1+E_1+I_1+R_1)(1+\mu^{\xi}\phi(h^{\xi}))=\phi(h^{\xi})\Lambda+c_1^{\xi}+q_1^{\xi}$$

$$(S_1+E_1+I_1+R_1)=\frac{\phi(h^{\xi})\Lambda+c_1^{\xi}+q_1^{\xi}}{1+\mu^{\xi}\phi(h^{\xi})}=N(N_1,\xi)$$

For $n=1$:

$$(S_2+E_2+I_2+R_2)(1+\mu^{\xi}\phi(h^{\xi}))=\phi(h^{\xi})\Lambda+c_1^{\xi}N(N_1,\xi)+c_2^{\xi}+q_2^{\xi}$$

$$(S_2+E_2+I_2+R_2)<\frac{\phi(h^{\xi})\Lambda+N(N_1,\xi)+c_1^{\xi}+q_1^{\xi}}{1+\mu^{\xi}\phi(h^{\xi})}=N(N_2,\xi)$$

For $n=2$:

$$(S_3+E_3+I_3+R_3)(1+\mu^{\xi}\phi(h^{\xi}))=\phi(h^{\xi})\Lambda+c_1^{\xi}N(N_2,\xi)+c_2^{\xi}+c_3^{\xi}+q_3^{\xi}$$

$$(S_3+E_3+I_3+R_3)<\frac{\phi(h^{\xi})\Lambda+N(N_2,\xi)+c_1^{\xi}+q_1^{\xi}}{1+\mu^{\xi}\phi(h^{\xi})}=N(N_3,\xi)$$

In the same way, it is true for $n=N_n$:

$$(S_n+E_n+I_n+R_n)<N(N_n,\xi)$$

Now, for $n\in\mathbb{Z}^+$ we have:

$$(S_{n+1}+E_{n+1}+I_{n+1}+R_{n+1})(1+\mu^{\xi}\phi(h^{\xi}))=\phi(h^{\xi})\Lambda+\sum_{i=1}^{n+1}p_i^{\xi}(S_{n+1-i}+E_{n+1-i}+I_{n+1-i}+R_{n+1-i})+q_{n+1}^{\xi}$$

$$(S_{n+1}+E_{n+1}+I_{n+1}+R_{n+1})<\frac{\phi(h^{\xi})\Lambda+N(N_n,\xi)+c_1^{\xi}+q_1^{\xi}}{1+\mu^{\xi}\phi(h^{\xi})}=N(N_{n+1},\xi)$$

As required.

4 Graphs

Here we will present the simulated graphs of the NVD model using the scheme proposed above,

4.1 Graphical Discussions

The graphical representations display the information at a glance. Here we will display the simulated graphs of the fractional NVD model by using the proposed numerical scheme. All graphs in Figure 1 reflect the evolution behavior of the solution variables in steady state without disease.

Figure 1 shows the progressive behavior of the susceptible population for different values of the fractional-order parameter ξ. The numerical templates designate the role of R_0 in the propagation of the disease. When R_0 is smaller than 1, the graphs successfully reach disease-free steady state, with different rates of convergence depending on the value ξ. For a greater value, the rate of convergence is higher as compared to smaller values and vice versa.

Similarly, the graphs for the infected, exposed, and recovered compartments converge towards the exact equilibrium point for $R_0<1$ and $\xi=0.9,0.8,0.7$, and 0.6, as described in the figures.

In the same vein, the graphs in Figure 2 display the convergence of the numerical graphs toward the endemic equilibrium point. For these graphs, it is mentioned that the value of R_0 is greater than 1, and the value of ξ is mentioned in the figures. All the graphs for every compartment converge towards the exact endemic steady state.

The graphs in Figure 3 exhibit the role of the awareness factor in virus propagation. It is observed that when a large number of susceptible individuals become aware of the disease dynamics, the number of exposed individuals reduces considerably while other parametric values are kept fixed.

The underlying fractional Nipah virus model exhibits a unique solution, local and global stability, and bounded properties. Moreover, the system has two steady states on which it is stable. Additionally, the mathematical model is well-posed, biologically meaningful, and significant. Our graphical templates illustrate all the features that are investigated analytically for the mathematical model. For instance, every graph converges toward the exact steady state preserving the positivity and boundedness. Moreover, the numerical scheme advocates the unique solution of the fractional NV model. Hence, our numerical scheme is physically in line with the mathematical model [28]-[36].

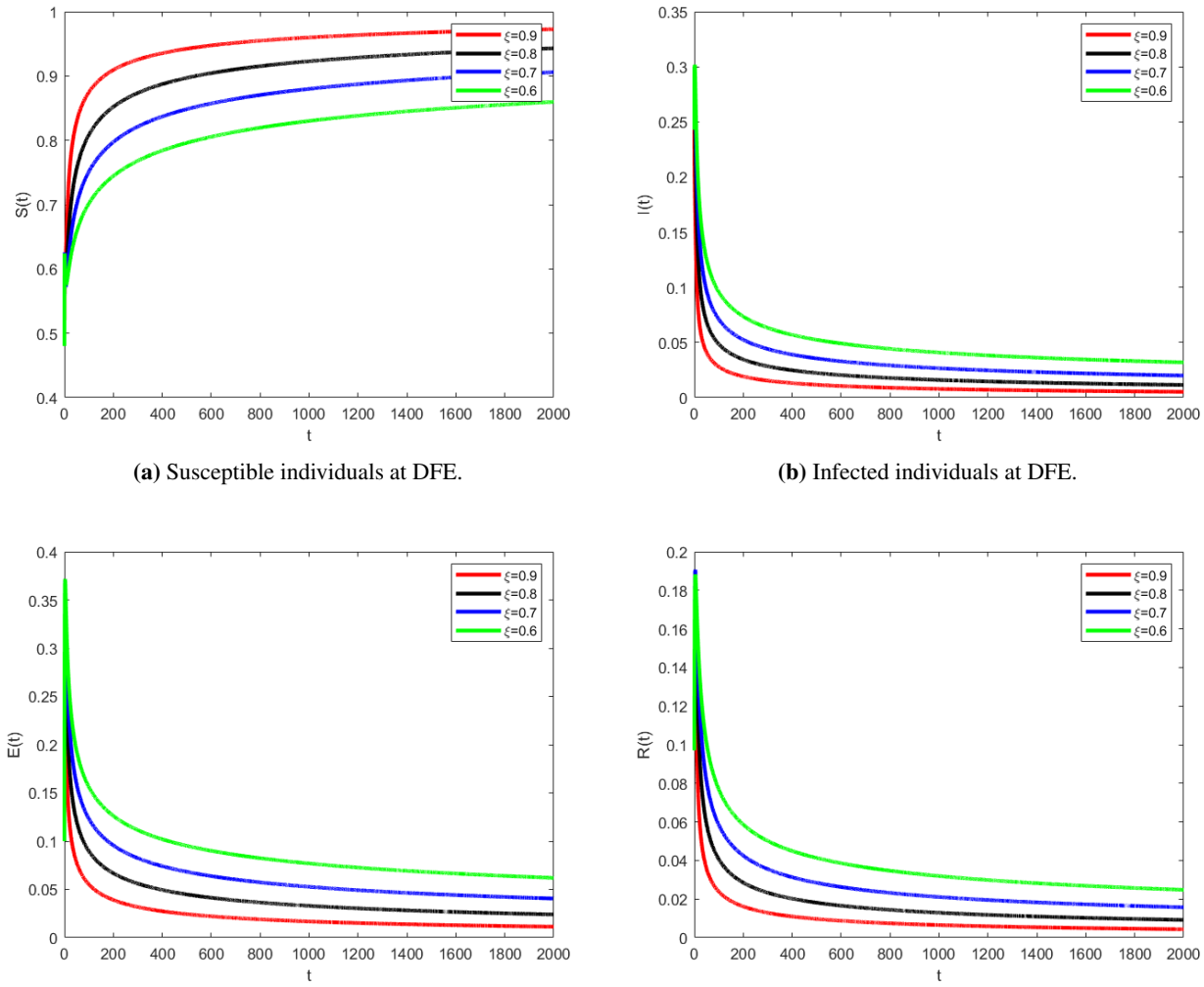

(a) Susceptible individuals at DFE.

(b) Infected individuals at DFE.

(c) Exposed individuals at DFE.

(d) Recovered individuals at DFE.

Fig. 1: The disease-free equilibrium points

5 Conclusion

In this study, we have converted the classical NVD model into the fractional-order NVD model to capture the Nipah virus disease dynamics. The extended model retains all the significant physical features of the disease dynamics. The NVD system has two dynamic steady states. Moreover, the system possesses local stability at both the fixed states of the fractional system. The system has only one solution, which indicates that the model is physically and biologically consistent and suitable for studying disease dynamics.

In addition, the fractional model has a positive and bounded solution for a definite time and non-negative initial conditions. For an approximate solution, the finite difference numerical method is designed to preserve the structure of the state variables. The finite difference numerical scheme is consistent with the fractional model. The novel numerical method guarantees a positive and bounded numerical solution. In addition, the design scheme converges to the true steady states of the underlying model.

The simulated graph reflects all the essential physical features of the solution variable. They reach the steady states depending on the value R_0. If the value of R_0 is less than 1, the graph converges towards the disease-free steady state, and if it is greater than 1, the graph of every state variable converges toward the endemic equilibrium point. Also, the

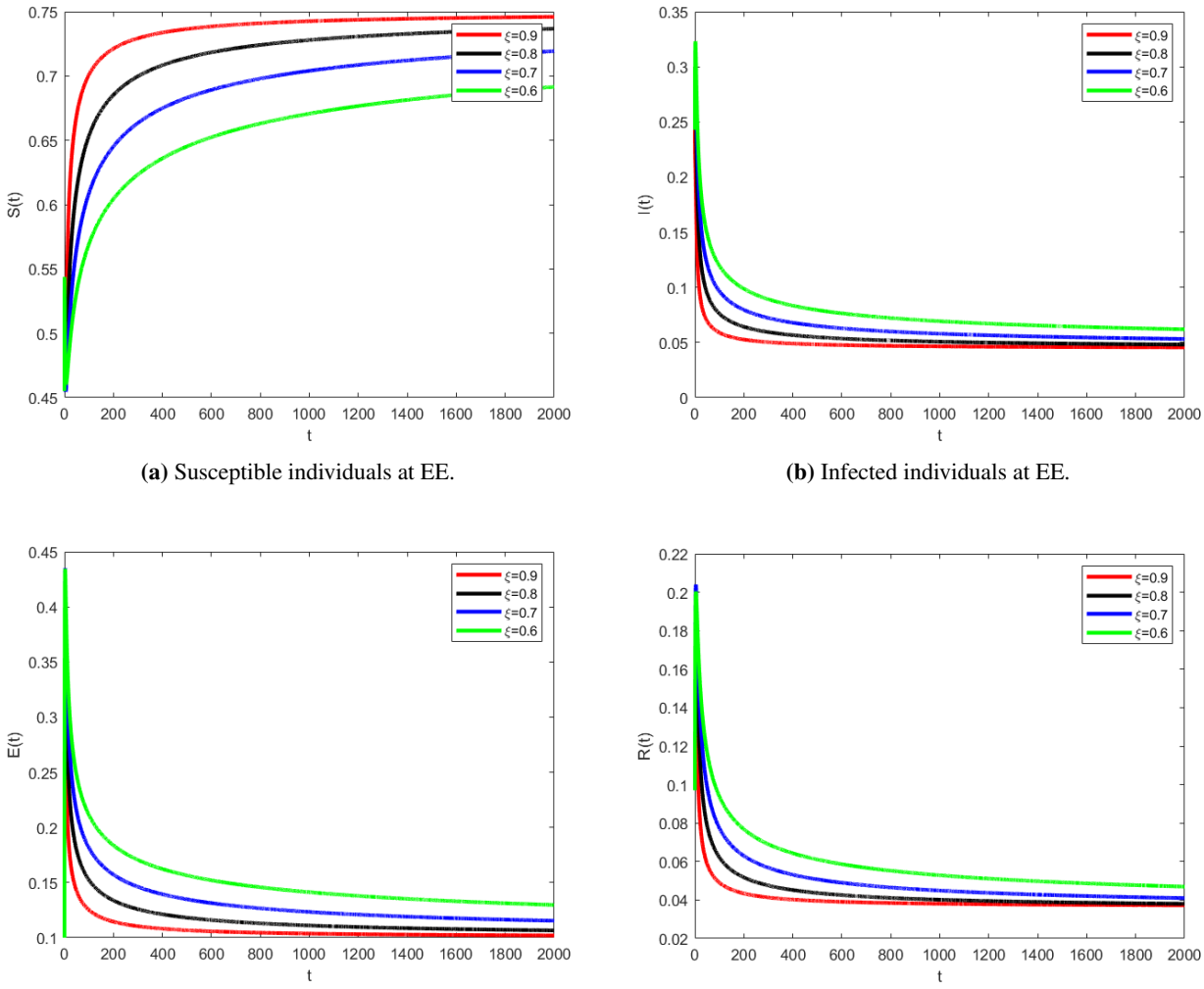

(a) Susceptible individuals at EE.

(b) Infected individuals at EE.

(c) Exposed individuals at EE.

(d) Recovered individuals at EE.

Fig. 2: The dissimilated graphs of endemic equilibrium

virus spreads quickly when R_0 is greater than 1 and diminishes when R_0 is less than 1. Consequently, all the results and simulated graphs demonstrate the novelty and efficacy of the projected numerical design.

The outcomes of this study are significant for predicting the NV disease, its peak time, and the possible duration of the NV among the population. Moreover, health resources may be allocated in a better way. Also, non-medical interventions such as social distancing, wearing face masks, etc. may be introduced among humans. Therefore, the study has a significant and physical impact on society.

Besides, the significance of the study has some potential limitations. For instance, the role of temperature and climate is not taken into account in the mathematical model. Similarly, the homogeneous mixing of infected individuals with the susceptible populace is not possible in real-world situations.

As a future perspective, this study may be applied to find the numerical solutions of various fractional non-linear epidemic models, predator-prey models, and chemical reaction-diffusion models.

Data Availability Statement

The data used in this research are taken from [23, 24, 26].

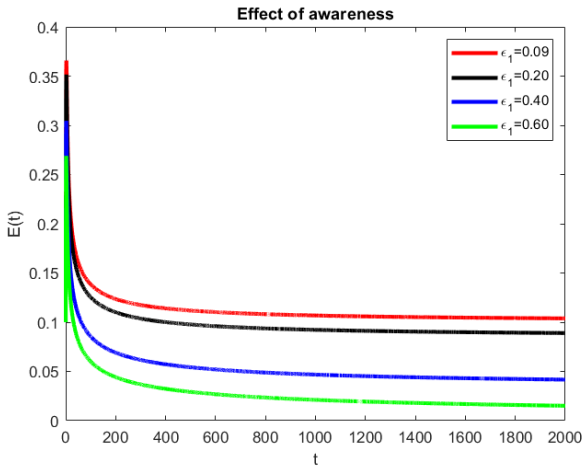

Fig. 3: effect of awareness on the exposed class

Authors Agreement

Authors are agreed to process the manuscript for review.

Acknowledgement

Conflict of Interest

The authors declare that there are no conflicts of interest regarding the publication of this paper.

Author Contributions

All authors have read and agreed to the published version of the manuscript.

Funding

No funding was received for this research.

References

[1] Yuen, K.Y.; Fraser, N.S.; Henning, J.; Halpin, K.; Gibson, J.S.; Betzien, L.; Stewart, A.J. Hendra virus: Epidemiology dynamics about climate change, diagnostic tests, and control measures. *One Health* **2021**, *12*, 100207.
[2] Mohd Nor, M.N.; Gan, C.H.; Ong, B.L. Nipah virus infection of pigs in peninsular Malaysia. *Rev. Sci. Tech.* **2000**, *19*, 160–165.
[3] Aditi; Shariff, M. Nipah virus infection: A review. *Epidemiol. Infect.* **2019**, *147*, e95.
[4] Thanapongtharm, W.; Linard, C.; Wiriyarat, W.; Chinsorn, P.; Kanchanasaka, B.; Xiao, X.; Biradar, C.; Wallace, R.G.; Gilbert, M. Spatial characterization of colonies of the flying fox bat, a carrier of Nipah virus in Thailand. *BMC Vet. Res.* **2015**, *11*, 81.
[5] Singh, R.K.; Dhama, K.; Chakraborty, S.; Tiwari, R.; Natesan, S.; Khandia, R.; Munjal, A.; Vora, K.S.; Latheef, S.K.; Karthik, K.; et al. Nipah virus: Epidemiology, pathology, immunobiology and advances in diagnosis, vaccine designing and control strategies—A comprehensive review. *Vet. Q.* **2019**, *39*, 26–55.
[6] Pillai, V.S.; Krishna, G.; Veettil, M.V. Nipah virus: Past outbreaks and future containment. *Viruses* **2020**, *12*, 465.
[7] Satterfield, B.A.; Dawes, B.E.; Milligan, G.N. Status of vaccine research and development for Nipah virus. *Vaccine* **2016**, *34*, 2971–2975.

[8] Devnath, P.; Wajed, S.; Chandra Das, R.; Kar, S.; Islam, I.; Masud, H.M.A.A. The pathogenesis of Nipah virus: A review. *Microb. Pathog.* **2022**, *170*, 105693.
[9] Pedrera, M.; Macchi, F.; McLean, R.K.; Franceschi, V.; Thakur, N.; Russo, L.; Medfai, L.; Todd, S.; Tchilian, E.Z.; Audonnet, J.C.; et al. Bovine herpesvirus-4-vectored delivery of Nipah virus glycoproteins enhances T cell immunogenicity in pigs. *Vaccines* **2020**, *8*, 115.
[10] Mungall, B.A.; Middleton, D.; Crameri, G.; Bingham, J.; Halpin, K.; Russell, G.; Green, D.; McEachern, J.; Pritchard, L.I.; Eaton, B.T.; et al. Feline model of acute Nipah virus infection and protection with a soluble glycoprotein-based subunit vaccine. *J. Virol.* **2006**, *80*, 12293–12302.
[11] Pallister, J.A.; Klein, R.; Arkinstall, R.; Haining, J.; Long, F.; White, J.R.; Payne, J.; Feng, Y.R.; Wang, L.F.; Broder, C.C.; et al. Vaccination of ferrets with a recombinant G glycoprotein subunit vaccine protects against Nipah virus disease for over 12 months. *Virol. J.* **2013**, *10*, 237.
[12] Weingartl, H.M.; Berhane, Y.; Caswell, J.L.; Loosmore, S.; Audonnet, J.C.; Roth, J.A.; Czub, M. Recombinant Nipah virus vaccines protect pigs against challenge. *J. Virol.* **2006**, *80*, 7929–7938.
[13] Yoneda, M.; Georges-Courbot, M.C.; Ikeda, F.; Ishii, M.; Nagata, N.; Jacquot, F.; Raoul, H.; Sato, H.; Kai, C. Recombinant measles virus vaccine expressing the Nipah virus glycoprotein protects against lethal Nipah virus challenge. *PLoS ONE* **2013**, *8*, e58414.
[14] Orusa, T.; Orusa, R.; Viani, A.; Carella, E.; Borgogno Mondino, E. Geomatics and EO data to support wildlife diseases assessment at landscape level: A pilot experience to map infectious keratoconjunctivitis in Chamois and phenological trends in Aosta Valley (NW Italy). *Remote Sens.* **2020**, *12*, 3542.
[15] Carella, E.; Orusa, T.; Viani, A.; Meloni, D.; Borgogno Mondino, E.; Orusa, R. An integrated, tentative remote-sensing approach based on NDVI entropy to model canine distemper virus in wildlife and to prompt science-based management policies. *Animals* **2022**, *12*, 1049.
[16] Kumar, V.B.; Rooney, N.; Carr, A. Nipah virus from bats—Another potential pandemic? Risk mapping the impact of anthropogenic and climate change on the transmission of Nipah virus infection to humans. *medRxiv* **2022**.
[17] Welbergen, J.A.; Klose, S.M.; Markus, N.; Eby, P. Climate change and the effects of temperature extremes on Australian flying foxes. *Proc. Biol. Sci.* **2008**, *275*, 419–425.
[18] Ratnayake, H.U.; Kearney, M.R.; Govekar, P.; Karoly, D.; Welbergen, J.A. Forecasting wildlife die-offs from extreme heat events. *Anim. Conserv.* **2019**, *22*, 386–395.
[19] Diengdoh, V.L.; Ondei, S.; Hunt, M.; Brook, B.W. Predicted impacts of climate change and extreme temperature events on the future distribution of fruit bat species in Australia. *Glob. Ecol. Conserv.* **2022**, *37*, e02181.
[20] European Union (EU). Regulation (EU) 2016/429 of the European Parliament and of the Council of 9 March 2016 on Transmissible Animal Diseases and Amending and Repealing Certain Acts in the Area of Animal Health ('Animal Health Law'). *Off. J.* **2016**. Available online: https://eur-lex.europa.eu/legal-content/EN/TXT/PDF/?uri=CELEX:32016R0429&from=EN (accessed on 22 December 2022)
[21] Aziz, B.J.; Azri, B.A. Nipah virus infection—Malaysia experience. In *Proceedings of the World Organization of Animal Health (OIE) Conference WILDLIFE ACTES 2011*; Available online: https://www.woah.org/fileadmin/Home/eng/Conferences_Events/sites/WILDLIFE_ACTES_2011/Presentations/S1_3_AzriBinAdzhar.pdf (accessed on 22 December 2022).
[22] National Centre for Disease Control (NCDC) India. Available online: https://ncdc.gov.in/ (accessed on 22 December 2022).
[23] Ahmed, N.; Elsonbaty, A.; Raza, A. et al. Numerical simulation and stability analysis of a novel reaction-diffusion COVID-19 model. *Nonlinear Dyn* **2021**, *106*, 1293–1310. https://doi.org/10.1007/s11071-021-06623-9.
[24] Mondal, M. K.; Hanif, M.; Biswas, M. H. A. A mathematical analysis for controlling the spread of Nipah virus infection. *International Journal of Modelling & Simulation* **2017**, *37*(3), 185–197. https://doi.org/10.1080/02286203.2017.1320820
[25] Arenas, A.J.; González-Parra, G.; Chen-Charpentier, B.M.; Construction of nonstandard finite difference schemes for the SI and SIR epidemic models of fractional order, *Math. Comput. Simulation* **2015**, *121*, 48-63.
[26] Raza, A.; Rafiq, M.; Ahmed, N.; Iqbal, M. S.; Rezapour, S.; Inc, M. Computer modeling: A gateway to novel advancements in solving real-life problems. *Biomed Signal Process Control* **2024** *95*, 106414.
[27] Manjunatha K.G., Chandrahasa C., Akshay S.D., Goh K.W., Comprehensive update on rabies: A neglected zoonotic disease of public health concern, *Progress In Microbes & Molecular Biology* (Volume 6, No.1, 2023, Pages 1 to 21)
[28] Liu, C., Liu, L., Cao, J., Abdel-Aty, M. (2023) Intermittent Event-Triggered Optimal Leader-Following Consensus for Nonlinear Multi-Agent Systems Via Actor-Critic Algorithm, IEEE Transactions on Neural Networks and Learning Systems, 34(8), pp. 3992–4006 http://dx.doi.org/10.1109/TNNLS.2021.3122458
[29] Wang, Z., Cao, J., Lu, G., Abdel-Aty, M. (2020) Fixed-Time Passification Analysis of Interconnected Memristive Reaction-Diffusion Neural Networks, IEEE Transactions on Network Science and Engineering, 7(3), pp. 1814–1824, 8906166 http://dx.doi.org/10.1109/TNSE.2019.2954463
[30] Wang, Z., Cao, J., Cai, Z., Abdel-Aty, M. (2020) A novel Lyapunov theorem on finite/fixed-time stability of discontinuous impulsive systems, Chaos, 2020, 30(1), 013139 http://dx.doi.org/10.1063/1.5121246
[31] Abdel-Aty, M., Moya-Cessa, H. (2007) Sudden death and long-lived entanglement of two trapped ions, Physics Letters A, 369(5-6), pp. 372–376 http://dx.doi.org/10.1016/j.physleta.2007.05.003
[32] Abdalla, M.S., Abdel-Aty, M., Obada, A.-S.F. (2002) Degree of entanglement for anisotropic coupled oscillators interacting with a single atom, Journal of Optics B 4(6), pp. 396–401 http://dx.doi.org/10.1088/1464-4266/4/6/305
[33] Abdel-Aty, M. (2002) General formalism of interaction of a two-level atom with cavity field in arbitrary forms of nonlinearities, Physica A 313(3-4), pp. 471–487 http://dx.doi.org/10.1016/S0378-4371(02)00999-8

[34] Abdalla, M.S., Obada, A.-S.F., Abdel-Aty, M. (2005) Von Neumann entropy and phase distribution of two mode parametric amplifier interacting with a single atom, Annals of Physics, 318(2), pp. 266–285 http://dx.doi.org/10.1016/j.aop.2005.01.002

[35] Abdel-Aty, M., Abdel-Khalek, S., Obada, A.-S.F. (2000) Pancharatnam phase of two-mode optical fields with Kerr nonlinearity, Optical Review, 7(6), pp. 499–504 http://dx.doi.org/10.1007/s10043-000-0499-6

[36] Obada, A.-S.F., Abdel-Hafez, A.M., Abdelaty, M. (1998) Phase properties of a Jaynes-Cummings model with Stark shift and Kerr medium, European Physical Journal D, 3(3), pp. 289–294 http://dx.doi.org/10.1007/s100530050176